Volume 3, Number 2, 2026

Pages 1171-1187

Bioscience Insights

ISSN: 3080-3489 (Print)
ISSN: 3080-3497 (Online)

BiosciInsights.com

EVALUATION OF SKELETAL METASTASES RELATED TO PRIMARY CANCERS USING BONE SCINTIGRAPHY AND SPECT/CT

Aisha Arif[1], Alizay Ijaz[2], Faryal Sadiq[3], Hadia Imran[4], Tanzila Aslam[5], Sadaf Abdul Qadir[*6]

[1,2,3,4,5]BS in Medical Imaging and Ultrasonography, University of Management and Technology, Lahore, Pakistan

*[*6]Assistant Professor, University of Management and Technology, Lahore, Pakistan*

*[*6]Master of Science in Medical imaging Technology, University of Management and Technology, Lahore, Pakistan*

[*6]sadaf.qadir@umt.edu.pk

https://doi.org/10.5281/zenodo.23117089

Article Information

Article History

Received:	May 15, 2026
Revised:	June 27, 2026
Accepted:	August 12, 2026
Available Online:	September 30, 2026

Keywords:
Skeletal Metastasis, Bone Scintigraphy, SPECT/CT, ^{99m}Tc-MDP, Primary Cancer, Imaging Diagnostics

Copyright @Author

Corresponding Author: *
Sadaf Abdul Qadir

Abstract

Bone metastasis is a clinically significant complication of advanced malignancy, and its prompt and accurate identification is essential for staging, treatment planning, and the prevention of skeletal-related events. Technetium-99m (^{99m}Tc) bone scintigraphy is the most widely used technique for whole-skeleton assessment, but planar images have limited specificity; hybrid single photon emission computed tomography/computed tomography (SPECT/CT) combines functional and anatomical information to improve lesion localization and characterization. This study aimed to evaluate skeletal metastases related to primary cancers using bone scintigraphy and SPECT/CT. A cross-sectional observational study was conducted over two months at the Combined Military Hospital (CMH), Lahore. Using convenience sampling, 59 adult patients with known primary malignancies referred for bone scintigraphy were enrolled; patients with primary bone tumors, severe renal impairment, recent trauma, fracture or orthopedic surgery, and pregnant or lactating women were excluded. Data were analyzed in SPSS version 26 using descriptive statistics, the chi-square test, Fisher's exact test, and McNemar's test. The mean age was 60.37 ± 15.36 years and the mean body weight 69.80 ± 7.72 kg, and 52.5% of patients were female. Breast (30.5%) and prostate (28.8%) cancers were the most common primary malignancies, and 69.5% of patients reported bone pain. Planar bone scintigraphy detected abnormalities in 44 patients (74.6%), whereas SPECT/CT detected abnormalities in 53 (89.8%). Every scintigraphy-positive patient was also positive on SPECT/CT, and SPECT/CT identified abnormalities in 9 of the 15 patients with negative planar scans. The spine, ribs, and pelvis were the most frequently involved sites. The

association between the two modalities was statistically significant ($\chi^2 = 19.59$, $p < 0.001$), and McNemar's test confirmed a significant difference in detection ($p = 0.004$). These findings indicate that bone scintigraphy remains a valuable screening tool, while the addition of SPECT/CT improves the detection, localization, and characterization of skeletal lesions and supports more accurate staging and treatment planning.

INTRODUCTION

Metastasis, the spread of cancer cells from the site of origin to distant tissues, represents the most advanced and aggressive stage of malignant disease and is responsible for the majority of cancer-related deaths. Tumor cells invade adjacent tissue, enter the blood or lymphatic circulation, and eventually colonize distant organs, where they may remain dormant or proliferate into secondary tumors. Because metastatic deposits often respond differently to systemic therapy than the primary tumor and frequently acquire treatment resistance, clinically established metastatic disease is, with few exceptions, incurable (Gerstberger, Jiang, & Ganesh, 2023). Although only a very small fraction of circulating tumor cells ultimately give rise to clinically significant metastases, metastatic disease accounts for approximately 90% of cancer deaths (Cook & Goh, 2020).

The skeleton is one of the most common sites of metastatic spread, and skeletal metastases are the most frequent malignant tumors of bone. Approximately 1.5 million people worldwide live with bone metastases, which weaken bone and predispose patients to pathological fracture, spinal cord compression, bone pain, and disability; these complications arise from tumor-induced disruption of normal bone remodeling, in which osteoclastic resorption and osteoblastic formation are normally balanced (Coleman, Brown, & Holen, 2020). Breast, prostate, and lung cancers show a particular predilection for bone, and up to 70% of patients with breast carcinoma may develop skeletal metastases. The spine, particularly the thoracic segment, is most often involved, followed by the ribs, pelvis, lower limbs, skull, sternum, shoulder girdle, and upper limbs (Yousef et al., 2024). Patients with bone metastases from common primaries such as breast and prostate cancer and multiple myeloma have an expected survival of only two to three years after diagnosis, largely owing to skeletal-related events such as hypercalcemia, pathological fracture, and nerve compression, which reduce both quality of life and overall survival (Zhang et al., 2021).

The predilection of metastases for the axial skeleton reflects the distribution of red, highly vascular marrow in the vertebrae, pelvis, ribs, sternum, skull, and proximal long bones, which facilitates extravasation and engraftment of circulating tumor cells. Approximately 70% of spinal metastases occur in the thoracic spine, 20% in the lumbosacral region, and 10% in the cervical spine, and proximal appendicular bones are involved more often than distal ones (Ban, Fock, Aryee, & Kovar, 2021). Bone metastases develop through a sequence of stages: homing of tumor cells to a pre-metastatic niche in the marrow, dormancy, reactivation, and finally alteration of osteoclast and osteoblast activity that produces the metastatic lesion (Ouvrard et al., 2024). On imaging, the resulting lesions are classified as osteolytic, osteoblastic (sclerotic), or mixed; renal cell, thyroid, and non-small cell lung carcinomas and non-Hodgkin's lymphoma most commonly produce osteolytic metastases, whereas prostate cancer characteristically produces sclerotic lesions (Migliorini et al., 2020).

Imaging is central to the diagnosis of skeletal metastases. Conventional radiography provides only two-dimensional information, whereas computed tomography (CT) and magnetic resonance imaging (MRI) offer detailed anatomical assessment, and scintigraphy and hybrid techniques such as positron emission tomography/computed tomography (PET/CT) and PET/MRI allow whole-body evaluation of both the morphological and functional properties of bone lesions (Rajakulasingam & Botchu, 2021; Shojaie et al., 2023) (Zafar et al., 2025) (Kanwal et al., 2026). Nuclear medicine imaging is particularly valuable because radiotracer uptake reflects cellular and molecular changes, allowing disease to be detected before structural abnormalities become apparent (Willowson & Bailey, 2026). A range of tracers, including ^{18}F-fluorodeoxyglucose (^{18}F-FDG), ^{18}F-sodium fluoride (^{18}F-NaF), and radiolabeled prostate-specific membrane antigen (PSMA) ligands, is now available, but ^{99m}Tc-labeled bisphosphonates have long

remained the mainstay of skeletal staging, particularly in breast and prostate cancer (Fan, Wang, Zou, & Liu, 2023; Zhao et al., 2020).

Bone scintigraphy with ^{99m}Tc-methylene diphosphonate (^{99m}Tc-MDP) or ^{99m}Tc-hydroxymethylene diphosphonate (^{99m}Tc-HDP) images sites of active osteoblastic bone formation. ^{99m}Tc has favorable properties for diagnostic imaging, including a physical half-life of 6.04 hours, monoenergetic 140 keV gamma emission, and rapid clearance, and approximately 50–60% of the injected diphosphonate is adsorbed to bone within 3–4 hours (Osman, Eltahry, Fawzy, & El-Sayed, 2022). The usual adult activity is 300–740 MBq, corresponding to an effective dose of approximately 2.9–4.2 mSv (Marshall, Prom-On, Sangkue, & Thiangsook, 2023). The technique is inexpensive, widely available, and safe, and it surveys the entire skeleton in a single examination (Huang et al., 2020). Its principal limitation is low specificity: fractures, osteoarthritis, degenerative joint and disc disease, and infection also increase osteoblastic activity and tracer uptake, while predominantly osteolytic or marrow-based lesions may be missed. In prostate cancer, the reported sensitivity and specificity of planar imaging are approximately 91% and 65%, respectively (Rohani et al., 2021).

Single photon emission computed tomography (SPECT) provides three-dimensional localization of radiotracer distribution, and since the introduction of hybrid scanners in 1999, SPECT/CT has combined functional SPECT data with the anatomical detail of co-registered CT (Bouchareb et al., 2024; Ritt, 2022) (Zafar, Fatima, et al., 2025) (Akbar et al., 2026). The CT component enables precise anatomical localization, attenuation correction, and differentiation of benign from malignant causes of tracer uptake on the basis of morphological features, and quantitative SPECT/CT now permits calculation of standardized uptake values (SUVs) as an imaging biomarker (Ikeda et al., 2022; Zamani-Siahkali et al., 2024) (Farooq et al., 2025). Compared with SPECT alone, SPECT/CT has been reported to increase diagnostic specificity from 78% to 89% without loss of sensitivity (Alqahtani, 2023), and whole-body SPECT/CT has demonstrated pooled sensitivity and specificity above 90%, with fewer equivocal findings than planar scintigraphy (Alqahtani, Fulton, Constable, Willowson, & Kench, 2020).

Bone metastases may mimic common orthopedic conditions, leading to delayed diagnosis, whereas early detection is essential for timely treatment and preservation of quality of life. Local data describing the pattern of skeletal metastases across different primary cancers and the incremental value of SPECT/CT over planar scintigraphy remain limited. It is anticipated that this study will clarify the distribution of skeletal involvement across primary malignancies and the added diagnostic value of hybrid imaging, supporting earlier diagnosis and better treatment planning. The objective of this study was to evaluate skeletal metastases related to primary cancers using bone scintigraphy and SPECT/CT.

Methodology

This cross-sectional, prospective observational study was carried out over a period of two months at the Combined Military Hospital (CMH), Lahore. A total of 59 patients with known primary malignancies who underwent whole-body bone scintigraphy with additional SPECT/CT imaging for suspected skeletal metastases were enrolled using a convenience sampling technique based on availability and eligibility.

Adults older than 20 years with a diagnosis of cancer who were referred for bone scintigraphy, who were able to give informed consent, and who had complete clinical records and previous imaging data were included. Patients with primary bone tumors, those unable to give consent, and those with severe renal impairment or recent trauma, fracture, or orthopedic surgery were excluded, as were pregnant or lactating women.

Data were collected using a structured proforma covering demographic details (age, gender, and body weight), type of primary cancer, time since cancer diagnosis, and clinical features, including the presence, location, duration, and severity of bone pain. Imaging data were obtained from the hospital's nuclear medicine database, electronic medical records, and Picture Archiving and Communication System (PACS). All whole-body bone scintigraphy and SPECT/CT examinations were performed on a dual-head gamma camera equipped with an integrated low-dose CT system according to the department's standard imaging protocol. For each modality, the presence or absence of skeletal abnormality and the anatomical distribution of lesions were recorded, together with the number of suspicious lesions on bone scintigraphy (single, 2–5, more than 5, or diffuse involvement), according to the final report issued by nuclear medicine specialists. Additional clinical information was obtained from the medical records where available to

corroborate the imaging results, and no further imaging or intervention was performed for the purpose of the study.

Data were entered into Microsoft Excel and analyzed using the Statistical Package for the Social Sciences (SPSS) version 26.0. Continuous variables were summarized as mean ± standard deviation and assessed for normality using the Kolmogorov–Smirnov and Shapiro–Wilk tests, and categorical variables were presented as frequencies and percentages. The association between abnormalities detected on bone scintigraphy and SPECT/CT was examined using the chi-square test and Fisher's exact test, and McNemar's test was used to compare the paired detection results of the two modalities; a p-value below 0.05 was considered statistically significant. The study was approved by the Institutional Review Board, written informed consent was obtained from every participant, and confidentiality of patient information was maintained throughout.

Results

This section reports the demographic and clinical characteristics of the 59 patients, followed by the findings of planar bone scintigraphy and SPECT/CT and the comparison between the two modalities. Descriptive distributions are presented in Tables 1–10, and normality testing and the association between the two modalities in Tables 11–13.

Demographic And Clinical Characteristics

Table 1. Descriptive statistics of patient age and weight.

Variable	N	Minimum	Maximum	Mean	SD
Age (years)	59	23	92	60.37	15.36
Weight (kg)	59	50	85	69.80	7.72

The mean age of the study population was 60.37 ± 15.36 years, ranging from 23 to 92 years, and the mean body weight was 69.80 ± 7.72 kg, ranging from 50 to 85 kg.

Table 2. Frequency and percentage of age group.

Age group	Frequency	Percent
21–30 years	8	13.6
31–40 years	2	3.4
41–50 years	7	11.9
51–60 years	13	22.0
61–70 years	10	16.9
71–80 years	14	23.7
81–90 years	4	6.8
91–100 years	1	1.7
Total	**59**	**100.0**

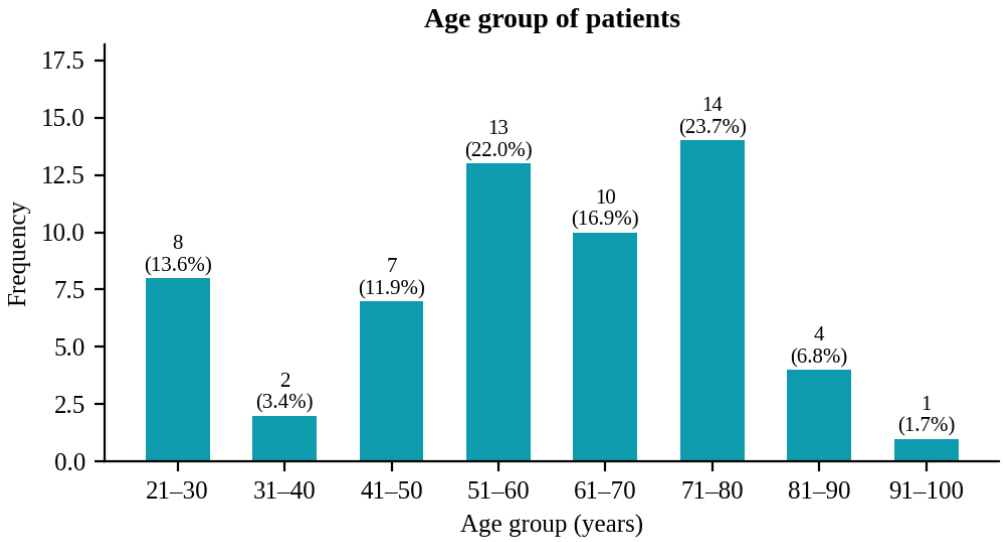


Figure 1. Frequency and percentage of age group.

The largest proportion of patients belonged to the 71–80-year age group (14, 23.7%), followed by the 51–60-year (13, 22.0%) and 61–70-year (10, 16.9%) groups. Patients aged 21–30 years accounted for 13.6% and those aged 41–50 years for 11.9%, while the 81–90-year (6.8%), 31–40-year (3.4%), and 91–100-year (1.7%) groups were least represented. The majority of patients were therefore older than 50 years.

Table 3. Frequency and percentage of gender.

Gender	Frequency	Percent
Female	31	52.5
Male	28	47.5
Total	**59**	**100.0**

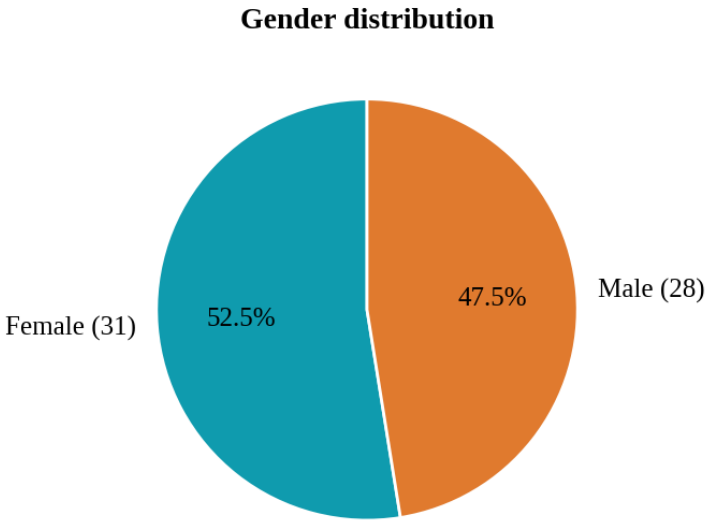


Figure 2. Frequency and percentage of gender.

Of the 59 patients, 31 (52.5%) were female and 28 (47.5%) were male, indicating a nearly equal representation of both genders with a slight female predominance.

Table 4. Distribution of patients according to type of primary cancer.

Primary cancer	Frequency	Percent
Breast	18	30.5
Prostate	17	28.8
Colon	8	13.6
Lung	7	11.9
Other	9	15.3
Total	**59**	**100.0**

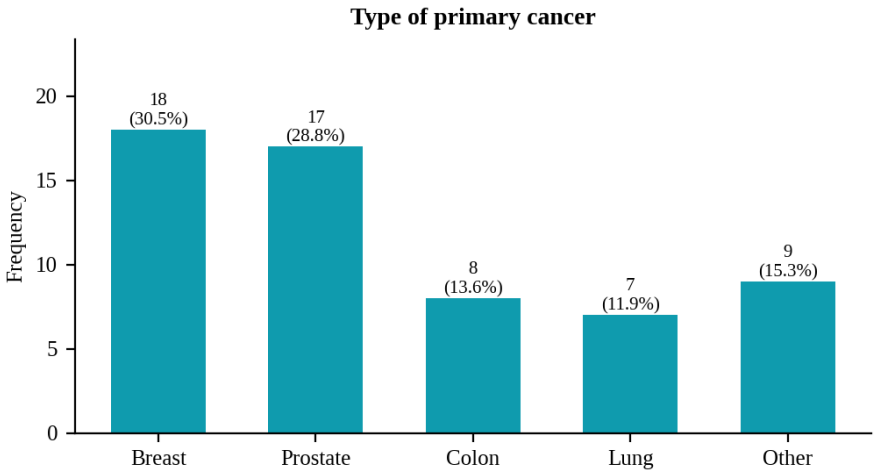


Figure 3. Distribution of patients according to type of primary cancer.

Breast cancer was the most common primary malignancy (18, 30.5%), followed closely by prostate cancer (17, 28.8%); together these two cancers accounted for 59.3% of the study population. Colon cancer was observed in 8 patients (13.6%), lung cancer in 7 (11.9%), and other malignancies in 9 (15.3%).

Table 5. Distribution of patients according to time since cancer diagnosis.

Time since diagnosis	Frequency	Percent
< 6 months	3	5.1
6–12 months	42	71.2
1–1.5 years	11	18.6
1.5–2 years	3	5.1
Total	**59**	**100.0**

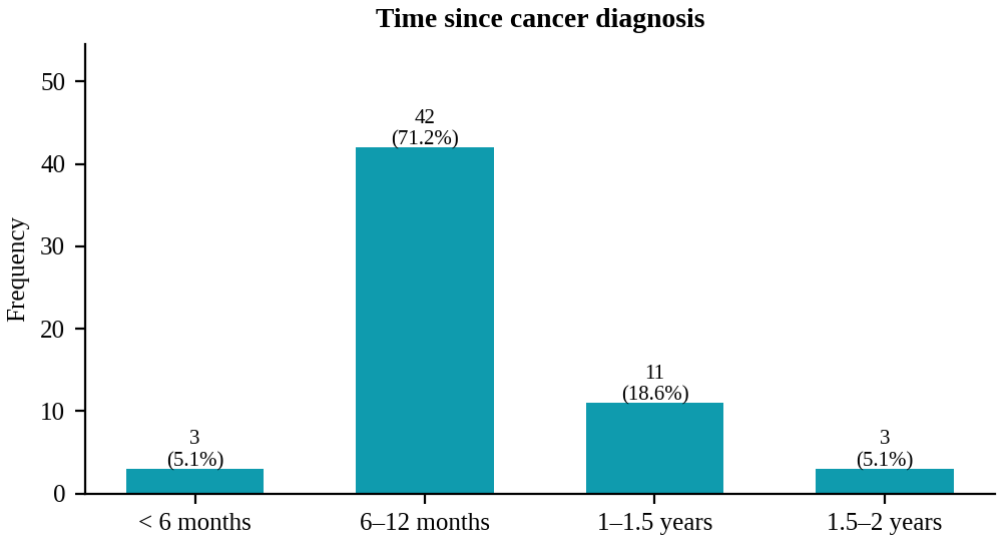


Figure 4. Distribution of patients according to time since cancer diagnosis.

Most patients (42, 71.2%) had been diagnosed with cancer 6–12 months before undergoing bone scintigraphy and SPECT/CT, and 11 (18.6%) had been diagnosed 1–1.5 years earlier. Only 3 patients (5.1%) had been diagnosed within the preceding six months, and another 3 (5.1%) had a cancer history of 1.5–2 years.

Table 6. Presence, duration, and severity of bone pain.

Variable	Category	Frequency	Percent
Bone pain	Present	41	69.5
	Absent	18	30.5
Duration of pain	< 1 month	3	5.1
	1–6 months	18	30.5
	> 6 months	20	33.9
	None	18	30.5
Severity of pain	Mild	9	15.3
	Moderate	26	44.1
	Severe	6	10.2
	None	18	30.5

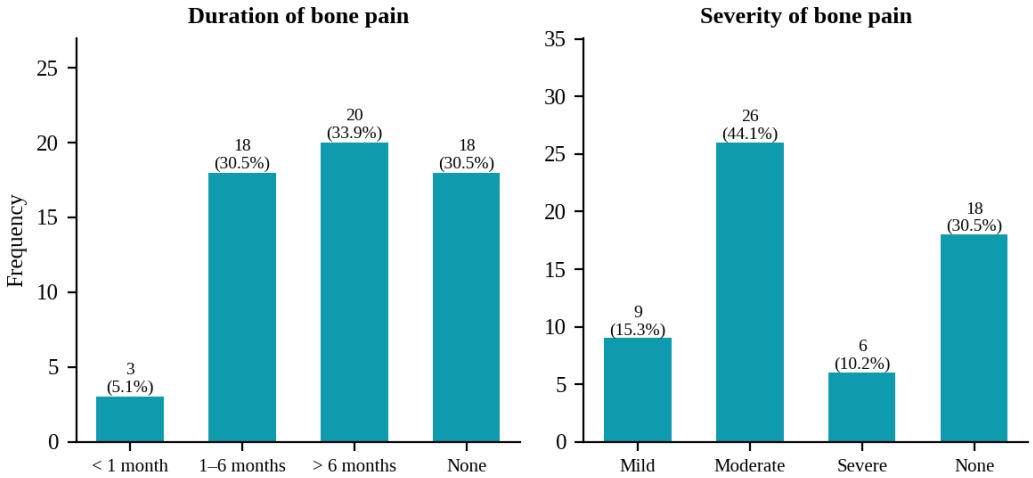


Figure 5. Duration and severity of bone pain.

Bone pain was the most commonly reported clinical feature, present in 41 patients (69.5%). Among these patients, pain had most often persisted for more than six months (20, 33.9%) or for 1–6 months (18, 30.5%), and only 3 patients (5.1%) reported pain of less than one month. Moderate pain predominated (26, 44.1%), while mild and severe pain were reported by 9 (15.3%) and 6 (10.2%) patients, respectively.

Table 7. Distribution of patients according to location of bone pain.

Location of pain	Frequency	Percent
Spine	5	8.5
Pelvis	1	1.7
Arms	1	1.7
Legs	3	5.1
Spine + pelvis	2	3.4
Spine + arms + legs	9	15.3
Arms + legs	4	6.8
Spine + pelvis + legs	2	3.4
Legs + pelvis	5	8.5
Ribs + arms + legs	9	15.3
None	18	30.5
Total	**59**	**100.0**

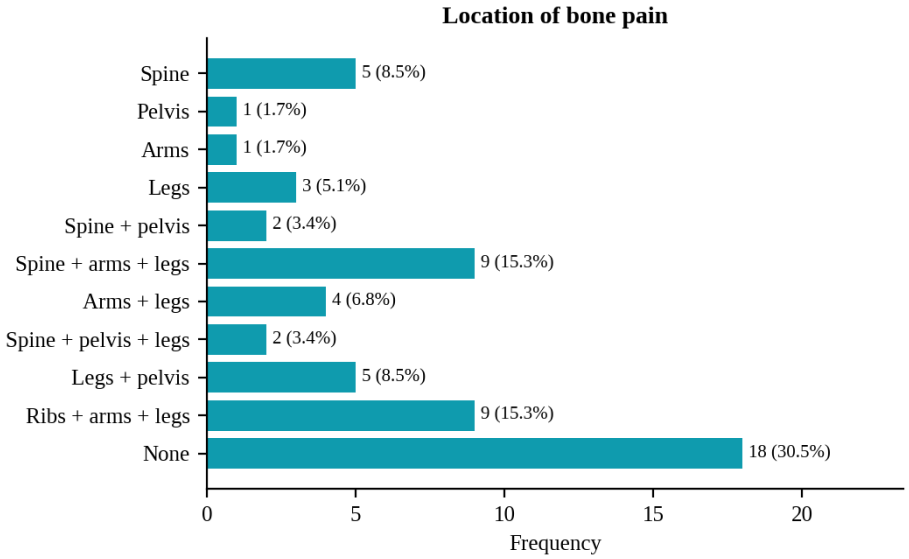


Figure 6. Distribution of patients according to location of bone pain.

Pain most frequently involved multiple regions: spine with arms and legs, and ribs with arms and legs, were each reported by 9 patients (15.3%). Isolated spinal pain and combined leg and pelvic pain were each reported by 5 patients (8.5%), and arm and leg pain by 4 (6.8%), whereas isolated leg, pelvic, and arm pain were uncommon.

Bone Scintigraphy and SPECT/CT Findings

Table 8. Abnormal findings detected on bone scintigraphy and SPECT/CT.

Finding	Bone scintigraphy, n (%)	SPECT/CT, n (%)
Abnormal	44 (74.6)	53 (89.8)
Normal	15 (25.4)	6 (10.2)
Total	**59 (100.0)**	**59 (100.0)**

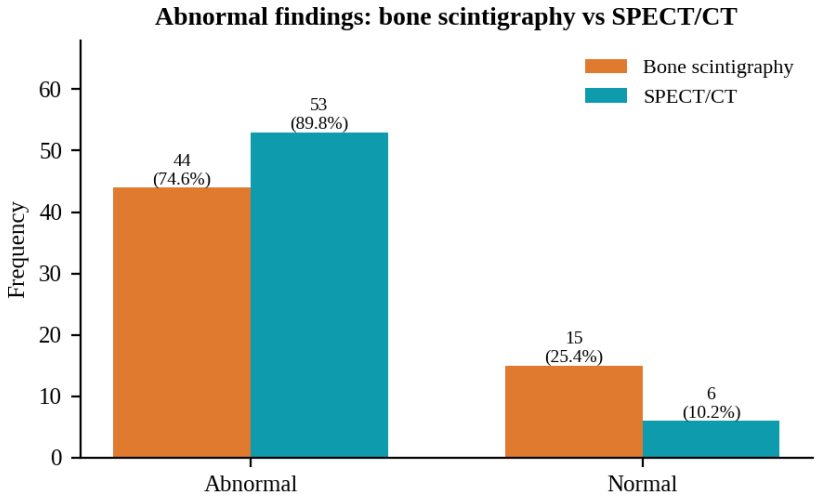


Figure 7. Abnormal findings detected on bone scintigraphy and SPECT/CT.

Planar bone scintigraphy demonstrated abnormal findings in 44 patients (74.6%), whereas SPECT/CT demonstrated abnormalities in 53 (89.8%). On SPECT/CT interpretation, all 53 abnormal studies showed metastatic lesions accompanied by coexisting degenerative changes, while the remaining 6 patients (10.2%) had no abnormal findings, reflecting the ability of the hybrid technique to separate malignant skeletal involvement from benign degenerative uptake.

Table 9. Number of suspicious lesions detected on bone scintigraphy.

Number of lesions	Frequency	Percent
Single lesion	3	5.1
2–5 lesions	25	42.4
> 5 lesions	12	20.3
Diffuse skeletal involvement	4	6.8
None	15	25.4
Total	**59**	**100.0**

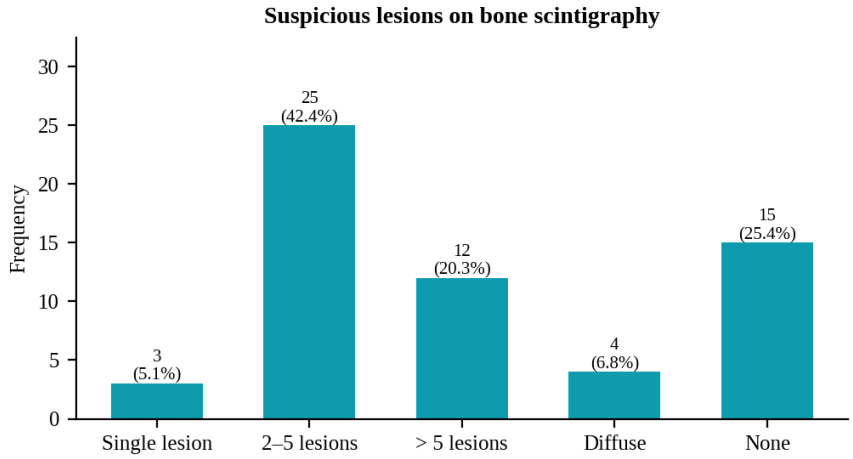


Figure 8. Number of suspicious lesions detected on bone scintigraphy.

Most patients with abnormal scans had multiple lesions: 25 (42.4%) had 2–5 suspicious lesions and 12 (20.3%) had more than five, while 4 (6.8%) showed diffuse skeletal involvement consistent with extensive metastatic disease. A solitary lesion was seen in only 3 patients (5.1%).

Table 10. Skeletal sites involved on bone scintigraphy and SPECT/CT.

Affected site(s)	Bone scintigraphy, n (%)	SPECT/CT, n (%)
Spine	5 (8.5)	6 (10.2)
Ribs	3 (5.1)	3 (5.1)
Pelvis	2 (3.4)	2 (3.4)
Spine + ribs + pelvis	5 (8.5)	6 (10.2)
LE + UE + head and neck	1 (1.7)	1 (1.7)
LE + UE + spine + pelvis	2 (3.4)	2 (3.4)
LE + UE + spine	5 (8.5)	5 (8.5)
Ribs + pelvis	6 (10.2)	11 (18.6)
UE + spine	3 (5.1)	3 (5.1)

Affected site(s)	Bone scintigraphy, n (%)	SPECT/CT, n (%)
LE + UE	2 (3.4)	2 (3.4)
LE + ribs + spine	5 (8.5)	7 (11.9)
Spine + ribs	5 (8.5)	5 (8.5)
None	15 (25.4)	6 (10.2)
Total	**59 (100.0)**	**59 (100.0)**

LE = lower extremities; UE = upper extremities.

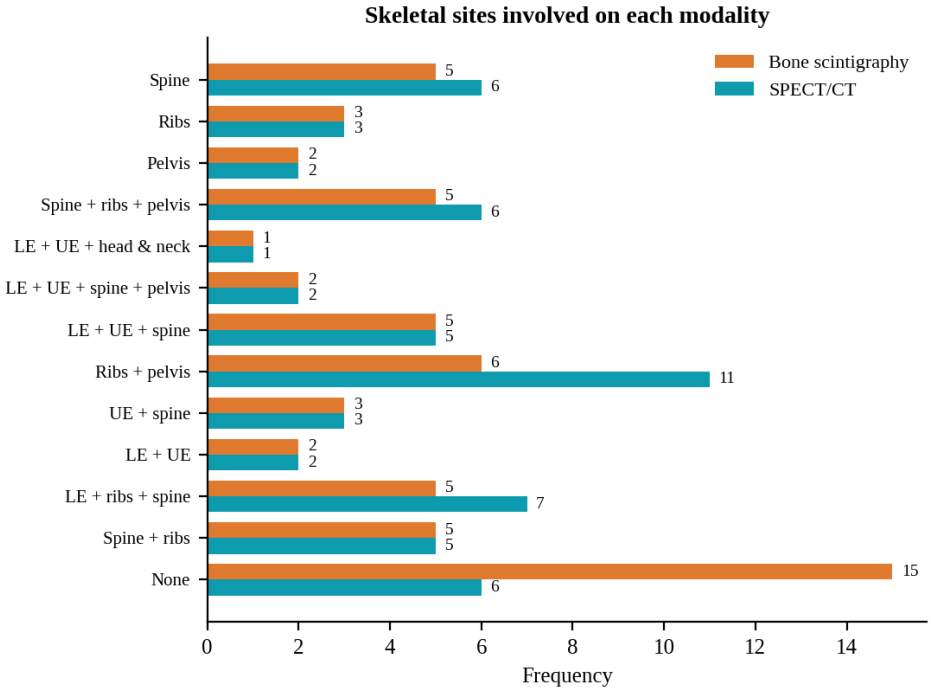


Figure 9. Skeletal sites involved on bone scintigraphy and SPECT/CT.

On bone scintigraphy, combined rib and pelvic involvement was the most frequent pattern (6, 10.2%), followed by isolated spinal involvement and several combinations involving the spine, ribs, and pelvis (5 each, 8.5%). SPECT/CT showed the same predominance of axial involvement with a higher number of positive findings: combined rib and pelvic involvement increased to 11 patients (18.6%), lower extremity, rib, and spinal involvement to 7 (11.9%), and isolated spinal and combined spine, rib, and pelvic involvement to 6 each (10.2%). The number of patients without skeletal involvement fell from 15 (25.4%) on bone scintigraphy to 6 (10.2%) on SPECT/CT.

Normality Testing and Association Between Modalities

Table 11. Tests of normality for continuous variables.

Variable	K–S statistic	K–S p-value	S–W statistic	S–W p-value
Weight	0.083	0.200	0.981	0.494
Age	0.085	0.200	0.977	0.327

K–S = Kolmogorov–Smirnov; S–W = Shapiro–Wilk; df = 59 for all tests.

Both patient weight (Kolmogorov–Smirnov p = 0.200; Shapiro–Wilk p = 0.494) and age (Kolmogorov–Smirnov p = 0.200; Shapiro–Wilk p = 0.327) had p-values greater than 0.05, confirming that the continuous variables were normally distributed.

Table 12. Cross-tabulation of abnormalities detected on bone scintigraphy and SPECT/CT.

Bone scintigraphy	SPECT/CT abnormal	SPECT/CT normal	Total
Abnormal	44	0	44
Normal	9	6	15
Total	**53**	**6**	**59**

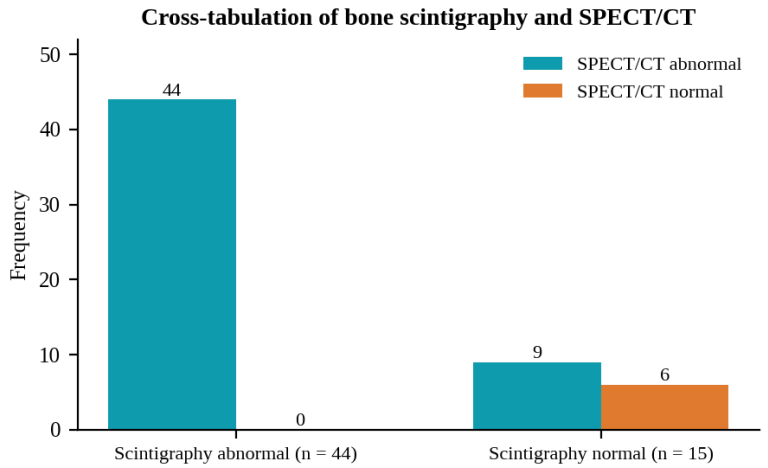


Figure 10. Cross-tabulation of abnormalities detected on bone scintigraphy and SPECT/CT.

All 44 patients (100%) with abnormalities on bone scintigraphy also demonstrated abnormal findings on SPECT/CT. Among the 15 patients with normal planar scans, 9 (60.0%) had abnormalities on SPECT/CT, and only 6 (40.0%) were negative on both modalities. No patient was positive on bone scintigraphy and negative on SPECT/CT.

Table 13. Chi-square and related tests for the association between bone scintigraphy and SPECT/CT findings.

Test	Value	df	p-value
Pearson chi-square	19.592	1	< 0.001
Continuity correction	15.458	1	< 0.001
Likelihood ratio	18.607	1	< 0.001
Fisher's exact test	—	—	< 0.001
Linear-by-linear association	19.260	1	< 0.001
McNemar test	—	—	0.004
N of valid cases	59		

The Pearson chi-square test demonstrated a statistically significant association between the findings of the two modalities (χ^2 = 19.592, df = 1, p < 0.001), which was supported by the likelihood ratio (χ^2 = 18.607, p < 0.001) and Fisher's exact test (p < 0.001). McNemar's test showed a statistically significant difference between the paired results (p = 0.004), indicating that SPECT/CT identified abnormalities that were not detected on planar bone scintigraphy.

Discussion

This study was conducted to evaluate skeletal metastases related to different primary cancers and to compare the findings of planar bone scintigraphy with those of hybrid SPECT/CT in the same patients. SPECT/CT identified skeletal abnormalities in 89.8% of patients compared with 74.6% on planar scintigraphy, detected every lesion-positive case seen on the planar images, and revealed additional involvement in patients whose planar scans were normal. Because both modalities were evaluated in the same individuals, these results directly demonstrate the added value of SPECT/CT for lesion detection, localization, and characterization in the assessment of skeletal metastases.

The patients in this study had a mean age of 60.37 years, and most were older than 50, with the 71–80-year and 51–60-year groups most represented. This is consistent with Yousef et al., who reported that the majority of 200 cancer patients referred for bone scintigraphy were older than 50 years and that older age is associated with a higher prevalence of cancer and bone metastases. The gender distribution in the present study was nearly equal (52.5% female, 47.5% male), whereas Yousef et al. reported a greater female proportion (60% female, 40% male); the more balanced distribution here probably reflects the similar numbers of breast and prostate cancer patients in the cohort. Both studies emphasize the importance of routine skeletal evaluation in elderly patients with cancer (Yousef et al., 2024).

Breast (30.5%) and prostate (28.8%) cancers were the most common primary malignancies, while colon (13.6%) and lung (11.9%) cancers were less frequent. This pattern agrees with the established epidemiology of bone metastasis, in which breast and prostate cancers have the strongest predilection for the skeleton; Yousef et al. likewise found breast and prostate cancer to be the leading primaries, with lung and colon cancer each accounting for 11% of cases. In both studies, the spine, ribs, and pelvis were the most frequently involved sites, and Zhou et al. similarly observed that abnormal radiotracer uptake in patients with pulmonary cancer was concentrated in the spine, pelvis, and bilateral ribs (Yousef et al., 2024; Zhou et al., 2024). This distribution reflects the abundant red marrow and rich vascular supply of the axial skeleton, which favor the seeding and growth of circulating tumor cells (Ban et al., 2021). The high proportion of patients with multiple lesions and the four patients with diffuse skeletal involvement further indicate that many patients presented with established, widespread metastatic disease; diffuse, intense skeletal uptake of this kind is recognized as a superscan pattern, most often associated with prostate cancer (Kovacsne, Kozon, Bentestuen, & Zacho, 2023).

The superior detection rate of SPECT/CT in the present study is consistent with the meta-analysis by Alqahtani et al., in which whole-body SPECT/CT achieved a patient-level sensitivity and specificity of 92–94% with an area under the curve of 0.99 and yielded fewer equivocal results than planar bone scintigraphy in eight of the included studies (Alqahtani et al., 2020). Arvola et al. similarly found reprojected bone SPECT/CT to be more sensitive than conventional planar scintigraphy for detecting metastases in breast and prostate cancer, albeit with somewhat lower specificity (Arvola et al., 2022). In a Pakistani prostate cancer patient, Parveen et al. showed that SPECT/CT clearly delineated extensive osteoblastic metastases in the lumbar spine, sacrum, pelvis, and proximal femora that could not be distinguished on planar images, enabling more accurate staging (Parveen, Fatima, Qureshy, & Shahid, 2023). In the present study, the 9 patients with normal planar scans but abnormal SPECT/CT findings represent 15.3% of the cohort who would otherwise have been under-staged.

Beyond detection, SPECT/CT improved lesion characterization. All 53 abnormal SPECT/CT studies contained both metastatic lesions and coexisting degenerative changes, a combination that commonly produces indeterminate uptake on planar imaging because degenerative disease also increases osteoblastic activity. The co-registered CT allows these benign changes to be distinguished from metastatic deposits on the basis of morphology, and Bouchareb et al. highlighted the advantages of SPECT/CT in lesion localization, attenuation correction, diagnostic confidence, and patient management (Bouchareb et al., 2024). Kapsoritakis et al. reported that targeted SPECT/CT reduced equivocal planar findings by 83.1%, thereby limiting the need for additional imaging and shortening the time to diagnosis (Kapsoritakis et al., 2021). Quantitative SPECT/CT offers further refinement: metastatic lesions show significantly higher SUVmax than degenerative lesions and normal bone (Ikeda et al., 2022; Kuji et al., 2017; Lin et al., 2023), and quantitative analysis has achieved sensitivities of 74–92% and specificities of 81–93% in differentiating benign from malignant bone lesions (Mutuleanu et al., 2023).

The statistically significant McNemar result (p = 0.004) confirms that the discordance between the two modalities was systematic rather than random, since every discordant case was positive on SPECT/CT and negative on planar imaging. These findings support the view of Suppiah et al. that SPECT/CT acquisition should, wherever feasible, become the standard approach to bone scintigraphy because it improves image quality, diagnostic confidence, and clinical usefulness (Suppiah et al., 2023). Nevertheless, SPECT/CT is not free of limitations. Zhang et al. reported a specificity of only 41.7% for combined whole-body scintigraphy and SPECT/CT against a pathological reference standard (Zhang et al., 2020), Li et al. concluded that SPECT/CT alone may be insufficient for complete evaluation of bone metastases in breast cancer and advocated SPECT/CT-guided biopsy (Li, An, & Zhang, 2022), and Kosmin et al. found whole-body MRI to be more sensitive than CT and bone scintigraphy for detecting early progression in bone-only metastatic breast cancer (Kosmin et al., 2020). The present study did not include a histopathological or follow-up reference standard, so the additional abnormalities detected on SPECT/CT should be interpreted as improved detection rather than confirmed diagnostic accuracy.
In summary, planar bone scintigraphy remains a sensitive and practical whole-body screening tool, but a meaningful proportion of skeletal involvement is detected or clarified only when SPECT/CT is added. The combination of functional and anatomical information provided by hybrid imaging supports more confident differentiation of metastatic from degenerative disease, more accurate staging, and more appropriate treatment planning in patients with known primary malignancies.

Conclusion

This study evaluated skeletal metastases in patients with various primary malignancies using planar bone scintigraphy and SPECT/CT. Breast and prostate cancers were the most common primary cancers associated with suspected bone metastases, and the spine, ribs, and pelvis were the most frequent sites of involvement. Planar bone scintigraphy proved useful for detecting metastatic lesions, but SPECT/CT increased the detection rate of abnormal findings from 74.6% to 89.8%, identified involvement in patients with normal planar scans, and helped distinguish metastatic lesions from coexisting degenerative changes. The addition of SPECT/CT to conventional bone scintigraphy can therefore facilitate timely clinical decisions, accurate staging, and optimized treatment planning in patients with suspected skeletal metastases.

Limitations of the Study

The study was conducted at a single tertiary care facility with a relatively small sample of 59 patients, which may limit statistical power and the generalizability of the findings to other settings. The heterogeneity of primary malignancies restricted analysis of cancer-specific subgroups. No histopathological or follow-up reference standard was available, so diagnostic accuracy measures such as sensitivity and specificity could not be calculated, and no long-term follow-up was performed to assess disease progression, treatment response, or survival. In addition, bone scintigraphy and SPECT/CT were not compared with other advanced modalities such as PET/CT or whole-body MRI.

Recommendations

Larger prospective multicenter studies with histopathological or clinical follow-up as a reference standard are recommended to validate these findings, to assess cancer-specific patterns of skeletal involvement, and to determine the diagnostic accuracy of each technique. Comparative studies including ^{18}F-NaF PET/CT, which may detect small bone metastases earlier than ^{99m}Tc-MDP imaging (Dadgar et al., 2022), and whole-body MRI are also needed to establish the most efficient imaging pathway. In clinical practice, SPECT/CT should be routinely performed in patients whose planar bone scintigraphy is equivocal or difficult to interpret, in order to improve lesion localization, diagnostic certainty, and clinical decision-making.

REFERENCES

Akbar, A., Aslam, A., Butt, M. A., Saddique, S., Munawar, A., Gillani, M. T., & Zafar, W. (2026). DIAGNOSTIC ACCURACY OF X-RAY COMPARED WITH COMPUTED TOMOGRAPHY FOR DETECTION OF NON-DISPLACED FRACTURES IN PAKISTAN. *Bioscience Insights*, *3*(02), 1-9.

Alqahtani, F. F. (2023). SPECT/CT and PET/CT, related radiopharmaceuticals, and areas of application and comparison. Saudi Pharmaceutical Journal, 31(2), 312–328.

Alqahtani, M., Fulton, R., Constable, C., Willowson, K., & Kench, P. (2020). Diagnostic performance of whole-body SPECT/CT in bone metastasis detection using ^{99m}Tc-labelled diphosphate: a systematic review and meta-analysis. Clinical Radiology, 75(12), 961.e11–961.e24.

Arvola, S., Seppänen, M., Malaspina, S., Mätzke, S., Raiko, J., Timonen, K. L., Ettala, O., Jambor, I., Anttinen, M., & Kuisma, A. (2022). Comparison of reprojected bone SPECT/CT and planar bone scintigraphy for the detection of bone metastases in breast and prostate cancer. Nuclear Medicine Communications, 43(5), 510–517.

Ban, J., Fock, V., Aryee, D. N., & Kovar, H. (2021). Mechanisms, diagnosis and treatment of bone metastases. Cells, 10(11), 2944.

Bouchareb, Y., AlSaadi, A., Zabah, J., Jain, A., Al-Jabri, A., Phiri, P., Shi, J. Q., Delanerolle, G., & Sirasanagandla, S. R. (2024). Technological advances in SPECT and SPECT/CT imaging. Diagnostics, 14(13), 1431.

Coleman, R., Brown, J., & Holen, I. (2020). Bone metastases. In Abeloff's Clinical Oncology (pp. 809–830). Elsevier.

Cook, G. J., & Goh, V. (2020). Molecular imaging of bone metastases and their response to therapy. Journal of Nuclear Medicine, 61(6), 799–806.

Dadgar, H., Norouzbeigi, N., Jokar, N., Zareizadeh, J., Gholamrezanezhad, A., Ahmadzadehfar, H., Abbaszadeh, M., & Assadi, M. (2022). Comparison of ^{18}F-NaF imaging, ^{99m}Tc-MDP scintigraphy, and ^{18}F-FDG for detecting bone metastases. World Journal of Nuclear Medicine, 21(1), 1–8.

Fan, Z., Wang, T., Zou, L., & Liu, D. (2023). Comparison of the diagnostic value of ^{18}F-NaF PET/CT and ^{99m}Tc-MDP SPECT for bone metastases: a systematic review and meta-analysis. Translational Cancer Research, 12(11), 3166.

Farooq, M. S. Y., Usman, M., Abid, D., Ali, N., Ashraf, S., Younas, M., & Zafar, W. (2025). Identification of Interstitial Lung Diseases in Smokers vs Non-Smokers Using HRCT. *Journal of Health, Wellness and Community Research*, e862-e862.

Gerstberger, S., Jiang, Q., & Ganesh, K. (2023). Metastasis. Cell, 186(8), 1564–1579.

Huang, J.-F., Shen, J., Li, X., Rengan, R., Silvestris, N., Wang, M., Derosa, L., Zheng, X., Belli, A., & Zhang, X.-L. (2020). Incidence of patients with bone metastases at diagnosis of solid tumors in adults: a large population-based study. Annals of Translational Medicine, 8(7), 482.

Ikeda, T., Kitajima, K., Tsuchitani, T., Takahashi, Y., Hama, Y., & Kotura, N. (2022). Effectiveness of quantitative bone SPECT/CT for bone metastasis diagnosis. Hellenic Journal of Nuclear Medicine, 25(3), 253–259.

Kanwal, L., Aimen, T., Zahra, B., Mustafa, A., Fatima, T., Faiz, S., & Zafar, W. (2026). Association of Computed Tomography (CT) Brain Findings with Neurological Symptoms in Non-Traumatic Patients. *Journal of Health, Wellness and Community Research*, 1-10.

Kapsoritakis, N., Stathaki, M., Bourogianni, O., Tsaroucha, A., Papadaki, E., Simos, P., & Koukouraki, S. (2021). Clinical impact of targeted single-photon emission computed tomography/computed tomography (SPECT/CT) bone scintigraphy on the assessment of bone metastasis in cancer patients. Nuclear Medicine Communications, 42(11), 1202–1208.

Kosmin, M., Padhani, A. R., Gogbashian, A., Woolf, D., Ah-See, M.-L., Ostler, P., Sutherland, S., Miles, D., Noble, J., & Koh, D.-M. (2020). Comparison of whole-body MRI, CT, and bone scintigraphy for response evaluation of cancer therapeutics in metastatic breast cancer to bone. Radiology, 297(3), 622–629.

Kovacsne, A., Kozon, I., Bentestuen, M., & Zacho, H. D. (2023). Frequency of superscan on bone scintigraphy: a systematic review. Clinical Physiology and Functional Imaging, 43(5), 297–304.

Kuji, I., Yamane, T., Seto, A., Yasumizu, Y., Shirotake, S., & Oyama, M. (2017). Skeletal standardized uptake values obtained by quantitative SPECT/CT as an osteoblastic biomarker for the discrimination of active bone metastasis in prostate cancer. European Journal of Hybrid Imaging, 1(1), 2.

Li, X., An, C., & Zhang, W. (2022). Is it sufficient to evaluate metastatic bone involvement in breast cancer using SPECT/CT? A new approach of SPECT/CT-guided targeted bone marrow biopsy. BMC Cancer, 22(1), 614.

Lin, L., Zheng, R., Geng, J., Wang, X., Li, M., Fan, R., Zheng, Y., & Yang, K. (2023). Skeletal standardized uptake values obtained using quantitative SPECT/CT for the detection of bone metastases in patients with lung adenocarcinoma. Frontiers in Medicine, 10, 1119214.

Marshall, S. K., Prom-On, P., Sangkue, S., & Thiangsook, W. (2023). Assessment of radiation exposure in a nuclear medicine department during ^{99m}Tc-MDP bone scintigraphy. Toxics, 11(10), 814.

Migliorini, F., Maffulli, N., Trivellas, A., Eschweiler, J., Tingart, M., & Driessen, A. (2020). Bone metastases: a comprehensive review of the literature. Molecular Biology Reports, 47(8), 6337–6345.

Mutuleanu, M.-D., Paun, D. L., Lazar, A. M., Petroiu, C., Trifanescu, O. G., Anghel, R. M., & Gherghe, M. (2023). Quantitative vs. qualitative SPECT-CT diagnostic accuracy in bone lesion evaluation—a review of the literature. Diagnostics, 13(18), 2971.

Osman, M. O., Eltahry, E. A., Fawzy, A. M. E. D., & El-Sayed, N. D. (2022). The role of whole-body SPECT/CT using Tc-99m MDP in characterization of osseous lesions in breast cancer patients. Egyptian Journal of Nuclear Medicine, 24(1), 52–64.

Ouvrard, E., Kaseb, A., Poterszman, N., Porot, C., Somme, F., & Imperiale, A. (2024). Nuclear medicine imaging for bone metastases assessment: what else besides bone scintigraphy in the era of personalized medicine? Frontiers in Medicine, 10, 1320574.

Parveen, A., Fatima, A., Qureshy, A., & Shahid, A. (2023). Diagnostic edge of SPECT/CT scintigraphy over planar bone imaging for detection of bone metastases in prostate cancer patients. Pakistan Journal of Nuclear Medicine, 13(1), 31.

Rajakulasingam, R., & Botchu, R. (2021). Current progress and future trends in imaging of musculoskeletal bone tumours. Journal of Clinical Orthopaedics and Trauma, 23, 101622.

Ritt, P. (2022). Recent developments in SPECT/CT. Seminars in Nuclear Medicine.

Rohani, M. F. M., Zanial, A. Z., Suppiah, S., Phay, K. P., Khan, F. M. A., Najib, F. H. M., Noor, N. M., Arumugam, M., Hassan, S. Z. A., & Vinjamuri, S. (2021). Bone single-photon emission computed tomography/computed tomography in cancer care in the past decade: a systematic review and meta-analysis as well as recommendations for further work. Nuclear Medicine Communications, 42(1), 9–20.

Shojaie, P., Afzali, M., Nischal, N., Iyengar, K. P., Yousef, M. M. A., & Botchu, R. (2023). Bone tumor imaging: an update on modalities and radiological findings. Journal of Arthroscopy and Joint Surgery, 10(3), 131–138.

Suppiah, S., Rohani, M. F. M., Zanial, A. Z., Shahrir, A. D. A., Khairuman, K. A., & Vinjamuri, S. (2023). A review on the usage of bone single-photon emission computed tomography/computed tomography in detecting skeletal metastases in the post-COVID-19 era: is it time to ditch planar and single-photon emission computed tomography only gamma camera systems? Indian Journal of Nuclear Medicine, 38(2), 191.

Willowson, K. P., & Bailey, D. L. (2026). Evolving SPECT-CT technology. British Journal of Radiology, 99(1183), 1271–1279.

Yousef, M., Algethami, S., Alfarra, R., Abdullah, B., Alahmadi, R., & Jastaniah, S. (2024). Bone metastasis evaluation using bone scintigraphy. Medicine and Biohealth Journal, 1(1).

Zafar, W., Fatima, A., Mukhtar, I., Maqsood, A., Nazakat, A., Khalid, A., & Inam, A. (2025). The Radiological Association of Renal and Ureteric Calculi with Hydronephrosis and Hydroureter on CT Scan. *Journal of Health, Wellness and Community Research*, e861-e861.

Zafar, W., Naveed, E., Fatima, N., Tariq, Z., Manzoor, A., Saeed, S., & Ghaffar, A. (2025). Myocardial Perfusion Imaging: An Approach to Find Out When to Add SPECT/CT in MIBI Scan. *Journal of Health, Wellness and Community Research*, e621-e621.

Zamani-Siahkali, N., Mirshahvalad, S. A., Farbod, A., Divband, G., Pirich, C., Veit-Haibach, P., Cook, G., & Beheshti, M. (2024). SPECT/CT, PET/CT, and PET/MRI for response assessment of bone metastases. Seminars in Nuclear Medicine.

Zhang, W., Bado, I. L., Hu, J., Wan, Y.-W., Wu, L., Wang, H., Gao, Y., Jeong, H.-H., Xu, Z., & Hao, X. (2021). The bone microenvironment invigorates metastatic seeds for further dissemination. Cell, 184(9), 2471–2486.e20.

Zhang, Y., Li, B., Wu, B., Yu, H., Song, J., Xiu, Y., & Shi, H. (2020). Diagnostic performance of whole-body bone scintigraphy in combination with SPECT/CT for detection of bone metastases. Annals of Nuclear Medicine, 34(8), 549–558.

Zhao, Z., Pi, Y., Jiang, L., Xiang, Y., Wei, J., Yang, P., Zhang, W., Zhong, X., Zhou, K., & Li, Y. (2020). Deep neural network based artificial intelligence assisted diagnosis of bone scintigraphy for cancer bone metastasis. Scientific Reports, 10(1), 17046.

Zhou, Y., Li, C., Jiang, S., Niu, F., Cui, F., Zhao, Y., Wei, D., Ma, H., & Li, Y. (2024). Diagnosis of SPECT/CT bone imaging combined with two serum examinations in patients with bone metastases from pulmonary cancer. Clinical and Translational Oncology, 26(1), 147–154.